Generation of supercontinuum bottle beam using an axicon

Ja-Hon Lin,[a] Ming-Dar Wei,[b] Hui-Hung Liang,[c] Kuei-Huei Lin,[d] and Wen-Feng Hsieh[c]

a)Department of Electro-Optical Engineering & In Institute of Electro-Optical Engineering
National Taipei University of Technology,Taipei 10608, Taiwan
b) Department of Photonics, Feng Chia University,
100, Wenhwa Rd., Seatwen, Taichung 407, Taiwan
c)Department of Photonics & Institute of Electro-Optical Engineering
National Chiao Tung University, 1001 Tahsueh Rd., Hsinchu 300, Taiwan
d)Department of Science, Taipei Municipal University of Education
1, Ai-Kuo West Rd., Taipei 100, Taiwan
mdwei@fcu.edu.tw
wfhsieh@mail.nctu.edu.tw

Abstract: A supercontinuum bottle beam was successfully produced by focusing a supercontinuum laser beam after passing through an axicon. The supercontinuum radiation was generated from a microstructured fiber pumped by a self-kerr-lens mode-locked femtosecond Ti:sapphire laser. The cross-section intensity distributions of the generated bottle were recorded by a beam profiler. Using the line filters to select different central wavelengths, the different colors of bottle beams show slightly different bottle ranges and diameters due to the dispersion of axicon and focusing lens. The results consist with the theoretical prediction using the Fresnel-Kirchhoff's formula in considering an incident Gaussian beam.

OCIS codes: (060.4370) Nonlinear optics, fiber; (030.1640) Coherence; (170.4520) Optical confinement and manipulation; (350, 5500) Propagation.

References and links

1. B. P. S. Ahluwalia, X.-C. Yuan, S. H. Tao, W. C. Cheong, L. S. Zhang, and H. Wang, "Micromanipulation of high and low indices microparticles using a microfabricated double axicon," J. Appl. Phys. **99**, 113104-1-113104-6 (2006).
2. B. P. S. Ahluwalia, W. C. Cheong, X.-C. Yuan, L.-S. Zhang, S.-H. Tao, J. Bu, and H. Wang, "Design and fabrication of a double-axicon for generation of tailorable self-imaged three-dimensional intensity voids," Opt. Lett. **31**, 987-989 (2006).
3. J. Yin and Y. Zhu, "LP01-mode output beam from a micro-sized hollow optical fiber: A simple theoretical model and its applications in atom optics," J. Appl. Phys. **85**, 2473-2481 (1999).
4. K. T. Gahagan and G. A. Swartzlander, "Optical vortex trapping of particles," Opt. Lett. **21**, 827-829 (1996).
5. J. Arlt and M. J. Padgett, "Generation of a beam with a dark focus surrounded by regions of higher intensity: the optical bottle beam," Opt. Lett. **25**, 191-193 (2000).
6. D. Yelin, B. E. Bouma, and G. J. Tearney, "Generating an adjustable three-dimensional dark focus," Opt. Lett. **29**, 661-663 (2004).
7. B. Lu, W. Huang, B. Zhang, F. Kong, and Q. Zhai, "Focusing properties of Bessel beams," Opt. Commun. **131**, 223-228 (1996).
8. S. Chavez-Cerda and G. H. C. New, "Evolution of focused Hankel waves and Bessel beams," Opt. Commun. **181**, 369-377 (2000).
9. J. C. Gutierrez-Vega, R. Rodriguez-Masegosa, and S. Chavez-Cerda, "Focusing evolution of generalized propagation invariant optical fields," J. Opt. A: Pure Appl. Opt. **5**, 276-282 (2003).
10. K. Ait-Ameur and F. Sanchez, "Gaussian beam conversion using an axicon," J. Modern Opt, **46**, 1537-1548 (1999).
11. P.-T. Tai, W.-F. Hsieh, and C.-H. Chen, "Direct generation of optical bottle beams from a tightly focused end-pumped solid-state laser," Opt. Express. **12**, 5827-5833 (2004).

#77358 - $15.00 USD Received 22 November 2006; revised 12 February 2007; accepted 1 March 2007

12. M. D. Wei, W. L. Shiao, and Y. T. Lin, "Adjustable generation of bottle and hollow beams using an axicon," Opt. Commun, **248**, 7-14 (2005).
13. D. A. Jones, S. A. Diddams, J. K. Ranka, A. Stentz, R. S. Windeler, J. L. Hall, and S. T. Cundiff, "Carrier-Envelope Phase Control of Femtosecond Mode-Locked Lasers and Direct Optical Frequency Synthesis," Science **288**, 635-649 (2000).
14. I. Hartl, X. D. Li, C. Chudoba, R. K. Ghanta, T. H. Ko, J. G. Fujimoto, J. K. Ranka, and R. S. Windeler, "Ultrahigh-resolution optical coherence tomography using continuum generation in an air–silica microstructure optical fiber," Opt. Lett. **26**, 608-610 (2001).
15. P. Li, K. Shi, and Z. Liu, "Manipulation and spectroscopy of a single particle by use of white-light optical tweezers," Opt. Lett. **30**, 156-158 (2005).
16. P. Li, K. Shi, and Z. Liu, "Optical scattering spectroscopy by using tightly focused Supercontinuum," Opt. Express **13**, 9039-9044 (2005).
17. P. Fischer, A. E. Carruthers, K. Volke-Sepulveda, E. M. Wright, C.T.A. Brown, W. Sibbett, and K. Dholakia, "Enhanced optical guiding of colloidal particles using a supercontinuum light source," Opt. Express **14**, 5792-5802 (2006).
18. J. Leach, G. M. Gibson, M. J. Padgett, E. Esposito, G. McConnell, A. J. Wright and J. M. Girkin, "Generation of achromatic Bessel beams using a compensated spatial light modulator," Opt. Express **14**, 5581-5587 (2006).
19. P. Fischer, C. T. A. Brown, J. E. Morris, C. López-Mariscal, E.M. Wright, W. Sibbett and K. Dholakia, White light propagation invariant beams," Opt. Express **13**, 6657-6666 (2005).
20. M.-L. Hu, C.-Y. Wang, E. E. Serebryannikov, Y.-J. Song, Y.-F. Li, L. Chai, K.V. Dukel'skii, A. V. Khokhlov, V. S. Shevandin, Y. N. Kondrat'ev, and A. M. Zheltikov , "Wavelength-tunable hollow-beam generation by a photonic-crystal fiber," Laser Phys. Lett. **3**, 306-309 (2006).
21. I. S. Gradshteyn and I. M. Ryzhik, "*Table of Integral, Series, and Products*", (Academic Press, New York, 1980).

1. Introduction

Recently, hollow beam and optical bottle beam have attracted great interests in various applications such as atom guiding, atom trapping and optical trapping of particles [1-4]. An optical bottle beam, in which a dark focus is surrounded by regions of higher intensity, has been produced by using a holographic plate [5] and interference of two laser beams with different curvatures [6]. Generation of bottle beams by focused Bessel beam are proposed, in which a ring image is generated in the focal plane of the lens, and a Bessel beam can also be reconstructed beyond the focal plane under particular focusing conditions [7-10]. The optical bottles can also be directly generated from a tightly focused end-pumped laser operated around the degenerate cavity configurations [11]. Recently, a dynamically one-parameter-tunable method with high-energy efficiency is used to generate various evolutions of beams [12]. The distance between the axicon and the focused lens is tuned to transform the focused beams from bottle beams to hollow beams that are experimentally demonstrated in consistent with theoretical predictions.

Supercontinuum (SC) generation by launching an ultrashort pulse into microstructure fibers (MFs) has been widely investigated due to their high nonlinear coefficient and tailorable dispersion. The generated SC has many practical applications, such as metrology, optical coherence tomography, and optical communication, etc. [13-14]. Besides, the generated SC has high spatial coherence that can be used for simultaneous micro-particle manipulation and spectroscopy in optical trapping [15-16]. Due to the chromatic aberration of lens, the enhanced spectral bandwidth of SC can elongate focal region in optical guiding of microscopic particles [17]. In use of the axicon [18] or spatial light modulator [19], the characteristics of white light Bessel beam were investigated, which can be used for the micromanipulation of atoms and mesoscopic particles. Wavelength tunable hollow-beam-generation from the dispersive wave through the MFs has been reported, which offers advantages for optical tweezers and atom guiding [20]. However, to our best knowledge, there are no reports on generating SC optical bottle beams.

In this work, we generate SC bottle beam by focusing a SC laser beam after passing through an axicon. Using line filters to select central wavelengths, the ranges of optical

#77358 - $15.00 USD Received 22 November 2006; revised 12 February 2007; accepted 1 March 2007

bottle beams of different wavelengths are measured. The experimental results consistent with the theoretical calculation using the Fresnel-Kirchhoff's formula in considering an incident Gaussian beam. This light source is expected to enhance trapping ability for the microparicles with different sizes, and different atoms required different blue detuning.

2. Experiments

The experimental setup is shown in Fig. 1. The output of femtosecond self-kerr-lens mode-locked (ML) Ti:sapphire laser was injected into a 90 cm-long MF (PM-760 from Crystal Fibre, Inc.) by a 40X microscope objective lens. The input pulsewidth and power of the ML Ti:sapphire laser are about 50 fs and 300 mW, respectively. The generated supercontinnum was collected and collimated by another 40X microscope objective lens. After the light passes through the axicon, the optical Bessel beam can be generated [6]. The axicon is made by the BK7 glass with an angle γ between the conical surface and flat surface of 5°. A convergent lens with focal length $f \sim 35$ mm (@ 632 nm) was put behind the axicon with a distance $z_0 \sim 7.2$ cm to generate optical bottle beam while z_0 is larger than f [12]. A beam imager (WinCamD, DataRay Inc.) was mounted on a translational stage to measure the spatial intensity distribution along the longitudinal distances z (the distance between the lens and beam profiler, as shown in Fig. 1). Three line filters with center wavelengths of 532, 670 and 780 nm (FL532-10, FL670-10, and FL780-10 with bandwidth of 10 nm from the ThorLab Inc.) were inserted between the microscope objective and the axicon, thus we could record the region of optical bottle beam at these wavelengths.

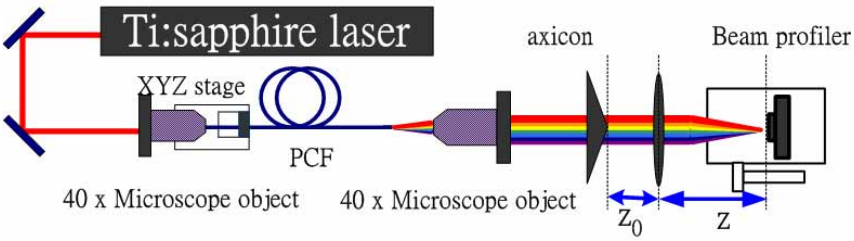

Fig. 1 Schematic diagram of the experimental setup for generating supercontinuum bottle beam.

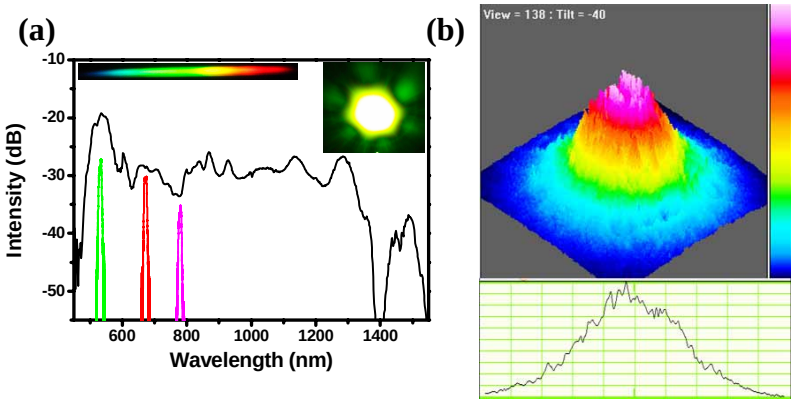

Fig. 2. (a). The spectra of the supercontinuum (black) and the selected band centered at 530 nm (green), 670 nm (red), and 780 nm (pink), respectively; inset are the photography of spanning visible spectra from the prism (upper left) and the output pattern from the MF (upper right). (b) The 3D intensity distribution (top) and its 1D radial intensity profile (bottom).

#77358 - $15.00 USD Received 22 November 2006; revised 12 February 2007; accepted 1 March 2007

3. Results and discussion

Figure 2(a) shows the generated SC from the MFs by optical spectral analyzer (Ando, AQ6315), with wavelength spanning from 460 nm to 1530 nm, and the photography of the spanning spectra dispersed by the prism, which shows the uniform distribution in the visible range [inset on the upper left of Fig. 2(a)]. The photography of the output mode pattern from the MF [the right inset of Fig. 2(a)] shows the hexagonal shape as predicted by the theoretical calculation. The measured 3D (top) and 1D (bottom) intensity distribution on the axicon in Fig. 2(b) shows the Gaussian-like distribution. Figure 3 show the cross section views of normalized 3D- and 1D-intensity distributions of the bottle beam as distance z increase [from Fig. 3(a) to Fig. 3(h)]. Figure 3(a) shows a sharp peak at the center of circular plateau that mainly results from a superposition of Gausian waves whose wave vectors are on the surface of a cone. Due to the dispersions of the axicon and the lens, different sizes of the rings were produced from Bessel-like beams for different center wavelengths, and the overlapping distribution does not exhibit a very clear Bessel-like ring. When z is set close to the near-end of central dark region, the central peak intensity falls as z increases. Then, the central peak intensity decreases below the plateau to become a dip as seen in Fig. 3(b), which is like a doughnut shape. Further increasing of z, the central dark region expands as shown in Fig. 3(c). Finally, the thinnest (the sharpest intensity) ring of optical bottle is formed at z = z_b = 34.58 mm, [Fig. 3(d)]. Getting further beyond this position, the reverse process appears that the ring expands with shrinking central dark region, as shown in Figs. 3(e) and 3(f). Finally, the intensity concentrates into the center to make dip become shallow in Fig. 3(g) and then become a peak again sitting on a base as in Fig. 3(h). A re-imaging of the far field of the Bessel beam to create the dark ring at the focus, the optical bottle is then closed axially on either side of the Bessel beam that can be simply explained geometrically in Fig. 1 of Ref. 12. When a Gaussian beam impinges through an axicon, a Bessel-Gaussian beam can be realized as a superposition of Gaussian beams whose wave vectors are on the surface of a cone. If we place a lens after the axicon, the oblique rays off axis through lens are focused to a spot away from axis at the focal plane. Laterally, all these spots assemble a doughnut beam shape and optical bottle in our experiment. In the neighbor before and after the region where bottle generates, the superposition of part of Gaussian beams forms a Bessel-like distribution. However, the Bessel-like distributions in this experiment on Figs. 3(a) and 3(h) were not clearly observed owing to the dispersion of the axicon and lens that makes different size of ring for each wavelength to cancel one another.

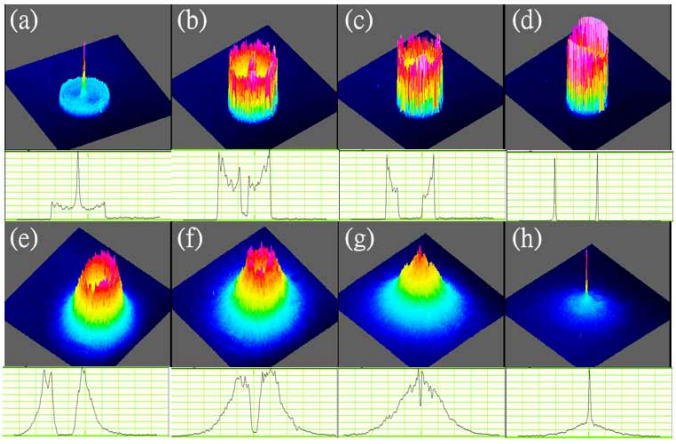

Fig. 3. The normalized 3D and 1D intensity distributions at (a) z = 26.20 mm, (b) z = 28.23 mm, (c) z = 32.09 mm, (d) z = 34.58 mm, (e) z = 40.27 mm, (f) z = 54.29 mm, (g) z = 59.12 mm, and (h) z = 64.50 mm.

#77358 - $15.00 USD Received 22 November 2006; revised 12 February 2007; accepted 1 March 2007

By inserting the line filter between the objective lens and axicon, a specific wavelength can be chosen to generate the monochromatic optical bottle beam. The variations of the diameters of the central doughnut dark region versus the distance z for the SC (squares), green (green triangles) are shown in Fig. 4. The photographs of the green and the red doughnut beam patterns are shown in the insets of Fig. 4. Due to the dispersion of the axicon and convergent lens, the distance $z = z_b$ from the convergent lens to the position where bottle beam has the thinnest ring and the largest diameter D_b of the dark region differs for various center wavelengths. The optical bottle beam with longer central wavelength has larger value of z_b and the smaller value of D_b for the dark region. By fitting the measured data in Fig. 4, we obtained the positions where the doughnut distributions begin at z_1 and terminate at z_2, and the lengths ($\Delta z = z_2 - z_1$) for the SC and different center wavelengths were all listed in Table 1. As the central wavelength becomes shorter, the range of bottle beam shifts toward the focusing lens and becomes shorter. Since all of the spectral components are included in the white-light bottle beam, it has the smallest range of bottle and the smallest diameter D_b in comparison with monochromatic bottle beam. Besides, the length Δz is adjustable if we vary the distance between the axicon and the lens z_0, as proposed in Ref. 12. The experimental layout provides a simple technique to generate an adjustable supercontinuum bottle beam.

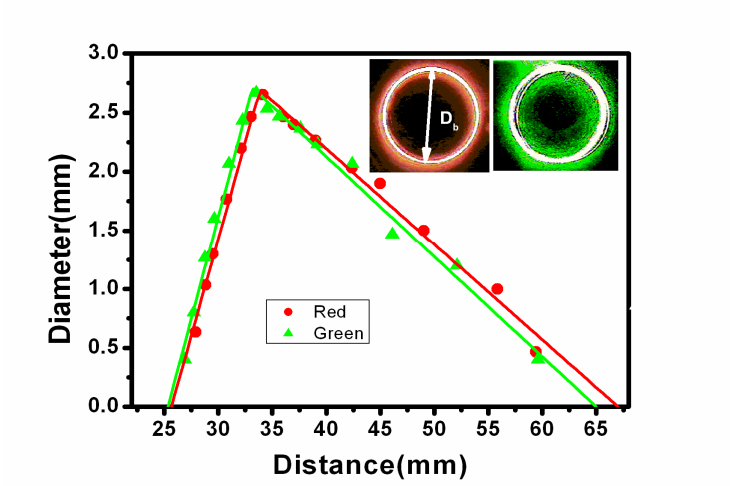

Fig. 4. Diameter variations of the dark region of the doughnut versus the distance z for the red light (red circles) and green light (green triangles).

Table.1 The measured (black) and calculated (red) range of bottle beam for the white-light SC, green light, red light, and IR.

	Z_1 (mm)	Z_b (mm)	D_b (mm)	Z_2 (mm)	ΔZ (mm)
White	26.31	34.58	2.62	64.41	38.10
Green(Exp/Cal)	25.34/25.33	33.50	2.66	65.01/65.79	39.67/40.46
Red (Exp/Cal)	25.66/25.57	34.12	2.65	67.01/66.84	41.35/41.27
IR (Exp/Cal)	25.93/25.71	34.35	2.63	67.59/67.27	41.66/41.56

#77358 - $15.00 USD Received 22 November 2006; revised 12 February 2007; accepted 1 March 2007

4. Theory

Tight assembly of an axicon and a positive lens can be used to transform a Gaussian beam either into a super-Gaussian, a ring-shape, or a doughnut-beam by changing the distance between them [10]. From the geometrical analysis of Ref. 12, the tightly assembled structure, i.e. $z_0 = 0$, can present a hollow beam beyond the lens only. In this section, we will focus on generation of the bottle beam by considering a Gaussian input beam passing through the separated assembly of an axicon and a lens. The transverse electric field distribution of the Gaussian beam with amplitude E_0 and radius W impinging on the axicon is given by

$$E_{in}(r) = E_0 \exp[-\frac{r^2}{w^2}]. \quad (1)$$

Here, the axicon has angle γ (between the conical and the flat surfaces) and reflective index n. After the Gaussian beam has passed through the axicon, it experiences a linear phase shift $\tau(r)=\exp(-ibr)$, where $b=2\pi n \tan(\gamma)/\lambda$ and λ is the wavelength of the incident beam. When we place a lens with the focal length f behind the axicon by a distance z_0, an optical bottle can be generated under the condition $z_0 > f$. The diffraction electric field amplitude $E(r',z')$ at a distance z' from the lens can be described by the Fresnel-Kirchhoff's formula as

$$E(r',z') = -\frac{2\pi i}{\lambda B} E_0 \exp(ikL) \exp\left(i\frac{kDr'^2}{2B}\right) \int_0^\infty \exp\left(-\frac{r^2}{W^2}\right) J_0\left(\frac{krr'}{B}\right) \exp\left(i\frac{kAr^2}{2B} - ibr\right) r dr, \quad (2)$$

where A, B, and D are the elements of the transform ABCD matrix of exiting from the axicon through the lens to the distance z'. Therefore, the on-axis electric field amplitude, i.e., $r'=0$ and $J_0(0)=1$, can be simplified to

$$E(0,z') = -\frac{2\pi i}{\lambda B} E_0 \exp(ikL) \int_0^\infty \exp\left(-\frac{r^2}{w^2}\right) \exp\left(i\frac{kAr^2}{2B} - ibr\right) r dr. \quad (3)$$

With the help of the integral formula of (3.462.5) in Ref. 21, we obtain the on-axis field

$$E(0,z') = -\frac{2\pi i}{\lambda B} E_0 \exp(ikL) \left\{ \frac{1}{2\mu} - \frac{ib}{4\mu}\sqrt{\frac{\pi}{\mu}} \exp\left(-\frac{b^2}{4\mu}\right) \left[1 - \Phi\left(\frac{ib}{2\sqrt{\mu}}\right)\right] \right\}. \quad (4)$$

Here, $\mu = \frac{1}{w^2} - i\frac{kA}{2B}$ and $\nu = i\frac{b}{2}$. Using the parameters $z_0 = 7.2$ cm, $W = 2.4$ mm, and refractive index n=1.51392 at 670 nm for Eq. (4), the on-axis intensity as a function of z' was plotted in Fig. 5. The focusing lens of different center wavelength will be considered and estimated by the formula $f = (n-1)/R$. We therefore can determine where the bottle begins and terminates (two foci) for different center wavelengths that are listed in red in Table 1. The values estimated from the theoretical calculation from Eq. (4) are close to the measured data that show shorter foci at the shorter central wavelength. The experimental results agree with theoretical predictions.

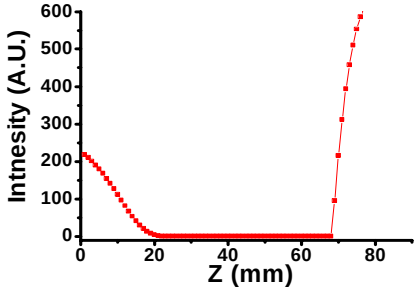

Fig. 5. The on-axis intensity of the optical bottle as a function of z.

#77358 - $15.00 USD Received 22 November 2006; revised 12 February 2007; accepted 1 March 2007

Practically, the smaller values of D_b about micron scale are required for optical trapping of microparticles. For example, low-index particles have been trapped by using a double axicon with γ =0.23° and 0.39° to produce optical bottle ~ 100 μm. Then, a telescope arrangement can further reduce the size of the bottle beam to about 10 μm [1-2]. In this experiment, we select the axicon with γ=5° to generate the optical bottle with lateral size of millimeter scale so that it can be easier to resolve by the beam imager. Based on the relation $D_b = f(n-1)\gamma$ [12], the lateral size of the optical bottle beam can be further reduced by selecting the focusing lens with larger NA or using the telescope systems. Unfortunately, the extreme rays may be attenuated by limiting NA to destroy the intensity structure of the generated bottle beam. Nevertheless, the axicon with smaller γ (< 0.25°) is commercially available such as those used in Refs. [12] and micro-fabrication of double axicon with γ = 0.1° and 0.08 ° [1-2] that can further reduce the size of the size (both axial and lateral) in micron scale. If we choose the axicon with smaller angle such as $\gamma = 0.25°$ and f = 2.5mm, we can simply estimate the lateral size D_b = 11.21 μm using the relation: $D_b = f(n-1)\gamma$ The value is close to numerically computed value of 11.19 μm using Eq. (2) with W = 150μm and $z_0 = f$ and the axial size is about 10 μm. Besides, the Bessel-Gaussian beam formed via a Gaussian beam's impinging through an axicon with smaller γ should have smaller divergent angle. As a result, the extreme rays being attenuated by limiting NA can also be avoided. Furthermore, in use of the various band-passed filters after lens, wavelength-adjustable bottle beams are selected to match the specific requirement for different atom trappings.

5. Conclusion

Supercontinuum bottle beam was successful produced by passing supercontinuum beam generated from microstructure fiber through assembly of axicon and positive-lens. Due to the dispersion of axicon and lens, the positions of two foci as well as the diameters of optical bottle depend on central wavelength. Thus, the range of the supercontinuum optical bottle is as predicted the smallest. In use of the Fresnel-Kirchhoff's formula and considering Gaussian input beam profile, the ranges of optical bottles at different center wavelengths are estimated, which is consistent with the measured results. We recognize that this light source can enhance trapping ability for the microscopic particles with slightly different sizes and different atoms required for different blue-detuning.

Acknowledgments

This work is supported by the National Science Council of Taiwan, Republic of China, under grant NSC-95-2221-E-009-308, NSC-95-2745-M-009-002, and NSC-95-2112-M-035-001. One of the authors, Dr. J.-H. Lin, would like to thank NSC 95-2811-M-009-002 for providing Postdoctoral fellowship.

#77358 - $15.00 USD Received 22 November 2006; revised 12 February 2007; accepted 1 March 2007